JOURNAL OF COMPUTATIONAL PHYSICS 54, 365–381 (1984)

Natural Convection in an Enclosed Cavity

TIMOTHY N. PHILLIPS

Institute for Computer Applications in Science and Engineering, NASA Langley Research Center, Hampton, Virginia 23665

Received March 8, 1983

We are concerned with the problem of buoyancy driven flow in a vertical, rectangular cavity whose vertical sides are at different temperatures and whose horizontal sides are insulated. An application of the dynamic A.D.I. method to obtain numerical solutions to this problem is described. For large non-dimensional temperature differences characterized by the Rayleigh number the flow patterns develop strong boundary layers. The boundary layers are resolved by applying the D.A.D.I. method to the discretization of this problem on a non-uniform grid.

1. INTRODUCTION

The problem to be considered was proposed by Jones [4] as a test bed for numerical methods for solving a variety of practical thermal problems. It is known as the "double glazing" or "window cavity" problem and has many applications, particularly in the field of thermal insulation. The most well-known application is double glazing, where a stagnant layer of air acts as an insulant between a warm room and a cold outside. The formulation of the problem is in terms of stream function, vorticity and temperature. The vorticity is eliminated to obtain a coupled pair of partial differential equations, one of which is fourth order. A dynamic A.D.I. (D.A.D.I.) method for solving these equations numerically is described. Grid stretching techniques originally due to Kalnáy de Rivas [8] are used to resolve the boundary layers which develop for large values of the Rayleigh number.

2. FORMULATION OF THE PROBLEM

We are concerned with the problem of fluid flow in an upright, rectangular cavity described in non-dimensional terms by $0 \leqslant x \leqslant 1$, $0 \leqslant z \leqslant 1$, with z vertically upward.

This research was supported in part by the Science and Engineering Research Council, United Kingdom, while the author was in residence at the Oxford University Computing Laboratory and Merton College, Oxford and in part by the National Aeronautics and Space Administration under Contract NAS1—17070, while the author was in residence at ICASE, NASA Langley Research Center, Hampton, Va. 23665.

0021-9991/84 $3.00

The cavity has different constant temperatures on the vertical walls, T_1 on the hot wall and T_2 on the cooler wall, and has insulated horizontal walls. We shall consider the two-dimensional flow of a Boussinesq fluid of Prandtl number 0.71 in which the flow takes place perpendicular to the walls. The Boussinesq approximation (see Mallinson and De Vahl Davis [9]) assumes that the physical properties and the density are constant except in the buoyancy term in the equations where the density is taken into account. This approximation is quite realistic and can give rise to predictions that are in good agreement with experiment (Jones [5]) for small temperature differences. The governing equations are considerably simplified by use of this approximation. A full discussion and detailed description of this problem is given by Jones [6].

A non-dimensional temperature, T, is defined by

$$T = \frac{(T^* - T_2)}{(T_1 - T_2)},$$

where T^* is the temperature. The equations representing the conservation of mass, momentum and energy may be written as

$$\nabla \cdot \mathbf{v} = 0, \tag{1}$$

$$(\nabla \times \mathbf{v}) \times \mathbf{v} = -\nabla p - \mathrm{Ra}\,\mathrm{Pr}\,T\mathbf{k} - \mathrm{Pr}\,\nabla^2 \mathbf{v}, \tag{2}$$

$$\nabla \cdot (\mathbf{v}T) = \nabla^2 T, \tag{3}$$

where $\mathbf{v} = (u, 0, w)$, $\mathbf{k} = (0, 0, 1)$ and p is the perturbation pressure. The Rayleigh number is given by

$$\mathrm{Ra} = g\beta(T_1 - T_2)/\kappa\nu$$

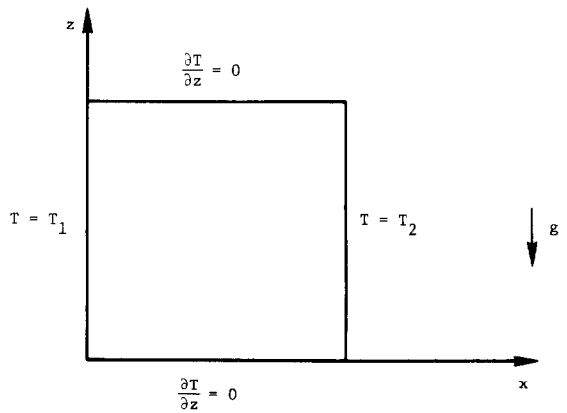

FIGURE 1

and the Prandtl number by

$$\mathrm{Pr} = \nu/\kappa,$$

where g is the acceleration due to gravity, β the coefficient of volumetric expansion, ν the coefficient of kinematic viscosity and κ the coefficient of thermal conductivity.

Mallinson and De Vahl Davis [10] show that the governing equations may be recast in the form

$$\mathrm{Pr}\,\nabla^2\zeta + \mathrm{Pr}\,\mathrm{Ra}\frac{\partial T}{\partial x} = u\frac{\partial \zeta}{\partial x} + w\frac{\partial \zeta}{\partial z}, \tag{4}$$

$$\nabla^2\psi = -\zeta, \tag{5}$$

$$\frac{\partial}{\partial x}(uT) + \frac{\partial}{\partial z}(wT) = \nabla^2 T, \tag{6}$$

$$u = -\frac{\partial \psi}{\partial z}, \qquad w = \frac{\partial \psi}{\partial x}, \tag{7}$$

where ζ is known as the vorticity and ψ the stream function. Equations (4) to (7) represent what is known as the vorticity–stream function formulation of the problem.

The boundary condition are

$$\psi = \frac{\partial \psi}{\partial n} = 0, \qquad \text{on} \quad \Gamma,$$

where Γ is the boundary of $\Omega = \{(x, z) : 0 \leqslant x \leqslant 1, 0 \leqslant z \leqslant 1\}$,

$$T = 1, \qquad \text{on} \quad x = 0,$$

$$T = 0, \qquad \text{on} \quad x = 1,$$

$$\frac{\partial T}{\partial n} = 0, \qquad \text{on} \quad z = 0 \text{ and } z = 1.$$

Eliminating the velocities u, w and the vorticity ζ we obtain the following system of equations:

$$\nabla^4\psi - \mathrm{Ra}\frac{\partial T}{\partial x} + \frac{1}{\mathrm{Pr}}\frac{\partial \psi}{\partial z}\frac{\partial}{\partial x}(\nabla^2\psi) - \frac{1}{\mathrm{Pr}}\frac{\partial \psi}{\partial x}\frac{\partial}{\partial z}(\nabla^2\psi) = 0, \tag{8}$$

$$\nabla^2 T - \frac{\partial}{\partial z}(wT) - \frac{\partial}{\partial x}(uT) = 0. \tag{9}$$

An advantage of eliminating the vorticity is that the need for a vorticity boundary condition is avoided. The system of equations (8) and (9) represents a fourth order equation for ψ and a second order equation for T. The major interest is in heat

transfer so there are two important quantities namely the temperature fields and the overall heat transfer defined by a Nusselt number

$$\mathrm{Nu} = \int_0^1 \frac{\partial T}{\partial x}\, dz \bigg|_{x=0}.$$

In order to solve this problem using an A. D. I. method we must first convert Eqs. (8) and (9) to the parabolic equations

$$\frac{1}{\lambda}\frac{\partial \psi}{\partial t} + \nabla^4 \psi - \mathrm{Ra}\frac{\partial T}{\partial x} + \frac{1}{\mathrm{Pr}}\frac{\partial \psi}{\partial z}\frac{\partial}{\partial x}(\nabla^2 \psi) - \frac{1}{\mathrm{Pr}}\frac{\partial \psi}{\partial x}\frac{\partial}{\partial z}(\nabla^2 \psi) = 0, \tag{10}$$

$$\frac{\partial T}{\partial t} = \nabla^2 T - \frac{\partial}{\partial x}(uT) - \frac{\partial}{\partial z}(wT), \tag{11}$$

whose steady state solution, if one exists, solves Eqs. (8) and (9). The parameter λ controls the interaction between the equations. It means that for $\lambda \neq 1$ we are effectively using different time scales for the two equations.

3. Solution of a Nonlinear Equation

In a numerical process to find the solution of Eqs. (8) and (9) we use Eq. 8 to solve for ψ and Eq. (9) to solve for T. Equation (8) is nonlinear with respect to ψ and can be written in the form

$$L(\psi) = f(T), \tag{12}$$

where L is a nonlinear operator.

A Newton-type method is used to solve Eq. (12). Suppose that ψ^* is some approximation to the solution of Eq. (12). We replace L by its linearization about ψ^* and then attempt to partially solve the linearized problem

$$L'(\psi^*) \cdot (\psi - \psi^*) + L(\psi^*) - f(T) \simeq 0, \tag{13}$$

where $L'(\psi^*)$ is the Frechet derivative of L at ψ^*. We use the D.A.D.I. method to solve Eq. (13), the linearization being updated after each D.A.D.I. step. This will be explained more fully later.

The Frechet derivative of L at ψ is given by

$$L'(\psi) \cdot \phi = \nabla^4 \phi + \frac{1}{\mathrm{Pr}}\frac{\partial \psi}{\partial z}\frac{\partial}{\partial x}(\nabla^2 \phi) + \frac{1}{\mathrm{Pr}}\left\{\frac{\partial}{\partial x}(\nabla^2 \psi)\right\}\frac{\partial \phi}{\partial z}$$

$$- \frac{1}{\mathrm{Pr}}\frac{\partial \psi}{\partial x}\frac{\partial}{\partial z}(\nabla^2 \phi) - \frac{1}{\mathrm{Pr}}\left\{\frac{\partial}{\partial z}(\nabla^2 \psi)\right\}\frac{\partial \phi}{\partial x}. \tag{14}$$

4. Finite Difference Equations

We cover Ω with a square grid of mesh length $h = 1/N$, where N is a positive integer. Let $\psi_{i,j}$ and $T_{i,j}$ be the values of ψ and T at the point (x_i, z_j), respectively, where $x_i = ih$ and $z_j = jh$. We use standard second-order centered difference approximations. At this point it is convenient to introduce the central difference operators δ_x^2 and $\bar{\delta}_x$ as follows:

$$\delta_x^2 v_{i,j} = v_{i+1,j} - 2v_{i,j} + v_{i-1,j}, \qquad \bar{\delta}_x v_{i,j} = v_{i+1,j} - v_{i-1,j}.$$

The central difference operators δ_z^2 and $\bar{\delta}_z$ are defined in a similar manner. Equations (8) and (9) are discretized using these approximations to give

$$\frac{1}{h^4}(\delta_x^4 + 2\delta_z^2\delta_x^2 + \delta_z^4)\psi_{i,j} - \frac{\mathrm{Ra}}{2h}\bar{\delta}_x T_{i,j} - \frac{1}{2h\,\mathrm{Pr}}(u_{i,j}\bar{\delta}_x p_{i,j} + w_{i,j}\bar{\delta}_z p_{i,j}) = 0, \tag{15}$$

and

$$\frac{1}{h^2}(\delta_x^2 + \delta_z^2)T_{i,j} - \frac{1}{2h}\bar{\delta}_x(uT)_{i,j} - \frac{1}{2h}\bar{\delta}_z(wT)_{i,j} = 0, \tag{16}$$

where

$$u_{i,j} = -\frac{1}{2h}\bar{\delta}_z\psi_{i,j}, \qquad w_{i,j} = \frac{1}{2h}\bar{\delta}_x\psi_{i,j}, \qquad p_{i,j} = \frac{1}{h^2}(\delta_x^2 + \delta_z^2)\psi_{i,j}.$$

The normal derivative boundary conditions are also discretized using central differences and these are used to remove imaginary exterior points from Eqs. (15) and (16) near the boundary. We have $2N(N-1)$ equations for the unknowns $\psi_{i,j}$, $i = 1,\ldots, N-1$, $j = 1,\ldots, N-1$, and $T_{i,j}$, $i = 1,\ldots, N-1$, $j = 0,\ldots, N$.

Equation (15) can be written in the form

$$L_h(\psi_{i,j}) = f_h(T_{i,j}),$$

which is the discrete form of Eq. (12), where L_h is a nonlinear discrete operator.

5. Method of Solution

Here we describe how the D.A.D.I. method of Doss and Miller [2] can be applied to this problem. Since Eqs. (10) and (11) are parabolic they may be advanced in time by a direct method and the complete solution procedure may be regarded as a single iterative scheme. Our interest is not in solving the parabolic equations (10) and (11)

accurately for finite times but to reach the steady state solution as soon as possible. We therefore use the D.A.D.I. method which uses a strategy that attempts to keep the time step Δt within a region of fast convergence. An advantage of using an automatic step size changer is that it avoids the necessity of choosing a priori iteration parameters. The strategy of Doss and Miller [2] attempts to recognize instabilites as they start to occur and to bypass them by decreasing Δt.

We start with initial approximations $T^{(0)}$ and $\psi^{(0)}$ to T and ψ, respectively, at time $t = 0$. Suppose that we have reached the nth time step, where $n = 2m$ and m is even, and that the current approximations of T and ψ at the grid points are $T^{(n)}$ and $\psi^{(n)}$, respectively. Starting from these approximations we describe a step of the D.A.D.I. method with time step Δt.

We begin by putting

$$\phi_{i,j}^{(n)} = 0,$$

for $i, j = 0, 1, \ldots, N$.

The A.D.I. scheme due to Peaceman and Rachford [11] is used to advance Eq. (11) in time. The following systems are solved along lines in the x-direction:

$$(r_1 I - \delta_x^2)\, T_{i,0}^{(n+1)} = (r_1 I + \delta_z^2)\, T_{i,0}^{(n)}, \qquad i = 1, \ldots, N-1, \tag{17}$$

$$\begin{aligned}(r_1 I - \delta_x^2)\, T_{i,j}^{(n+1)} + \tfrac{1}{2} h \bar{\delta}_x (u^{(n)} T^{(n+1)})_{i,j} \\ = (r_1 I + \delta_z^2)\, T_{i,j}^{(n)} - \tfrac{1}{2} h \bar{\delta}_z (w^{(n)} T^{(n)})_{i,j}, \qquad i = 1, \ldots, N-1,\ j = 1, \ldots, N-1,\end{aligned} \tag{18}$$

$$(r_1 I - \delta_x^2)\, T_{i,N}^{(n+1)} = (r_1 I + \delta_z^2)\, T_{i,N}^{(n)}, \qquad i = 1, \ldots, N-1, \tag{19}$$

with

$$T_{0,j}^{(n+1)} = 1, \qquad T_{N,j}^{(n+1)} = 0, \qquad j = 0, 1, \ldots, N,$$

homogeneous Neumann boundary conditions along $z = 0$ and $z = 1$ and where $r_1 = h^2/\Delta t$.

The following systems are solved along lines in the z-direction:

$$\begin{aligned}(r_1 I - \delta_z^2)\, T_{i,j}^{(n+2)} + \tfrac{1}{2} h \bar{\delta}_z (w^{(n)} T^{(n+2)})_{i,j} \\ = (r_1 I + \delta_x^2)\, T_{i,j}^{(n+1)} - \tfrac{1}{2} h \bar{\delta}_x (u^{(n)} T^{(n+1)})_{i,j}, \qquad j = 0, \ldots, N,\ i = 1, \ldots, N-1,\end{aligned} \tag{20}$$

with homogeneous Neumann boundary conditions along $z = 0$ and $z = 1$.

We advance ψ in time using the A.D.I. scheme of Douglas and Rachford [3] to solve the fourth order linear equation (13). The extension of this scheme to solve the biharmonic equation is due to Conte and Dames [1].

We solve the following systems, described by $j = 1, \ldots, N-1$, along lines in the x-direction:

$$\left\{r_2 I + \delta_x^4 + \frac{1}{4\mathrm{Pr}}(\bar{\delta}_z \psi_{i,j}^{(n)})\,\bar{\delta}_x \delta_x^2 - \frac{1}{4\mathrm{Pr}}[\bar{\delta}_z(\delta_x^2 + \delta_z^2)\,\psi_{i,j}^{(n)}]\,\bar{\delta}_x\right\}\phi_{i,j}^{(n+1)}$$

$$= \left\{r_2 I - \delta_z^4 - 2\delta_z^2\delta_x^2 - \frac{1}{4\mathrm{Pr}}[\bar{\delta}_x(\delta_x^2 + \delta_z^2)\,\psi_{i,j}^{(n)}]\,\bar{\delta}_z\right.$$

$$\left. + \frac{1}{4\mathrm{Pr}}(\bar{\delta}_x \psi_{i,j}^{(n)})\,\bar{\delta}_z(\delta_x^2 + \delta_z^2) - \frac{1}{4\mathrm{Pr}}(\bar{\delta}_z \psi_{i,j}^{(n)})\,\bar{\delta}_x \delta_z^2\right\}\phi_{i,j}^{(n)}$$

$$+ L_h(\psi_{i,j}^{(n)}) - f_h(T_{i,j}^{(n)}), \qquad i = 1,\ldots, N-1, \tag{21}$$

with homogeneous Dirichlet and Neumann boundary conditions, and where $r_2 = h^4/(\lambda \Delta t)$.

The following equations, described by $i = 1,\ldots, N-1$, are solved along lines in the z-direction:

$$\left\{r_2 I + \delta_z^4 - \frac{1}{4\mathrm{Pr}}(\bar{\delta}_x \psi_{i,j}^{(n)})\,\bar{\delta}_z \delta_z^2 + \frac{1}{4\mathrm{Pr}}[\bar{\delta}_x(\delta_x^2 + \delta_z^2)\,\psi_{i,j}^{(n)}]\,\bar{\delta}_z\right\}\phi_{i,j}^{(n+2)}$$

$$= \left\{\delta_z^4 - \frac{1}{4\mathrm{Pr}}(\bar{\delta}_x \psi_{i,j}^{(n)})\,\bar{\delta}_z \delta_z^2 + \frac{1}{4\mathrm{Pr}}[\bar{\delta}_x(\delta_x^2 + \delta_z^2)\,\psi_{i,j}^{(n)}]\,\bar{\delta}_z\right\}\phi_{i,j}^{(n)}$$

$$+ r_2 \phi_{i,j}^{(n+1)}, \qquad j = 1,\ldots, N-1. \tag{22}$$

We define an A.D.I. step to be the process by which we obtain $T^{(n+2)}$ and $\phi^{(n+2)}$ from $T^{(n)}$ and $\phi^{(n)}$, i.e., the solution of equations (17) to (22). Starting with the approximations $T^{(n+2)}$ and $\phi^{(n+2)}$ we perform a second A.D.I. step using the same time step Δt to obtain $T^{(n+4)}$ and $\phi^{(n+4)}$. The next part of the process is the bookkeeping stage of the D.A.D.I. step. Here we start with the approximations $T^{(n)}$ and $\phi^{(n)}$ and perform an A.D.I. step with time step $2\Delta t$ to obtain $\tilde{T}^{(n+4)}$ and $\tilde{\phi}^{(n+4)}$. We compute the test parameter, TP, which is given by

$$TP = \sqrt{|SUM/ASUM|},$$

where

$$SUM = \|T^{(n+4)} - \tilde{T}^{(n+4)}\|_2^2 + \|\phi^{(n+4)} - \tilde{\phi}^{(n+4)}\|_2^2$$

and

$$ASUM = \|T^{(n+4)} - T^{(n)}\|_2^2 + \|\phi^{(n+4)} - \phi^{(n)}\|_2^2.$$

The test parameter is an estimate of the relative local truncation error. If we are interested in solving the parabolic equations (10) and (11) accurately then Δt will be small, and so will TP. Our main concern, however, is to accelerate convergence and attempt to push TP into an interval where convergence for A.D.I. is rapid.

The process for computing TP requires that we solve each step twice which means that the number of computations is multiplied by 3/2. However the advantages of

having an automatic step size changer which decreases Δt when instabilities occur and attempts to keep Δt within a region of fast convergence seem to outweigh this extra computation.

The strategy for changing Δt given below is described in Doss and Miller [2]. In their paper Doss and Miller give theoretical justification of this strategy for a model problem. Although their analysis of the step size strategy rests on rigid assumptions, they obtain good results in situations where these no longer hold. If $TP > 0.6$ then we reject the present D.A.D.I. step and start the step again with Δt reduced by a factor of $1/16$. If $TP \leqslant 0.6$ then we accept the present D.A.D.I. step and change Δt according to the strategy: if TP falls in the intervals $[0, 0.05]$, $(0.05, 0.1]$, $(0.1, 0.3]$, $(0.3, 0.4]$, $(0.4, 0.6]$ change Δt by the factors 4, 2, $\sqrt{3}$, $\frac{1}{2}$, $\frac{1}{4}$ respectively for the next D.A.D.I. step.

If the present step is accepted then we use one step of Newton's method to update the approximation to ψ by setting

$$\psi^{(n+4)} = \psi^{(n)} - \phi^{(n+4)}.$$

We are now in a position to start the next D.A.D.I. step.

We note that the method described here contains all the ingredients required for a Richardson extrapolation, i.e.,

$$T_{\text{extrap}}^{(n+4)} = \alpha T^{(n+4)} + (1-\alpha)\,\tilde{T}^{(n+4)},$$
$$\phi_{\text{extrap}}^{(n+4)} = \alpha \phi^{(n+4)} + (1-\alpha)\,\tilde{\phi}^{(n+4)},$$

with the proper choice of α. Experiments were performed with this variation of the method and the results are reported later.

6. Numerical Results

The initial approximations $T^{(0)}$ and $\psi^{(0)}$ are chosen to be the values at the grid points of the functions T_I and ψ_I, respectively, where

$$T_I(x, y) = 1 - x, \qquad \psi_I(x, y) = 0.$$

The initial time step was chosen to be 10^{-4} in all cases. The algorithm described in the previous section was run for different grid sizes and for Rayleigh numbers of 10^3, 10^4, 10^5, and 10^6. The algorithm is terminated when the maximum modulus of the difference between successive iterates on even time steps is less than 10^{-6} for $h = 1/16$, $1/32$ and 5×10^{-5} for $h = 1/64$.

We experimented with different values of the parameter λ. For $\lambda = 1$ we found that for large values of the Rayleigh number the iterates oscillated. Mallinson and De Vahl Davis [9] also experience this kind of behavior and give the following explanations for it. First, there is an upper limit on the usable time step when solving a system which is generally not the case with a single equation. Second, if this

TABLE I

Variation of Number of D.A.D.I. Steps with λ^{-1}

λ^{-1}	Number of D.A.D.I. steps
50	433
100	125
200	111
350	86
500	111
1000	190
2000	318

stability condition is violated the instabilities can be controlled if λ is reduced which means that the effective Δt for one of the equations can be increased above this limit if that for the other equation is reduced. This suggests that the oscillations which would develop in the absence of a stability limit or without a reduction in λ must be due to an interaction between the equations. For suitable choices of this parameter the instabilities were controlled and the method converged. The value of λ^{-1} was chosen to be 20, 100, 500 and 500 respectively for Rayleigh numbers of 10^3, 10^4, 10^5 and 10^6. These values of λ^{-1} were determined by performing experiments on coarse grids. The choice of λ^{-1} was not critical in the sense that similar convergence behavior was observed for a wide range of values in the neighborhood of the chosen value. This can be seen in Table I, where we show the dependence of the number of D.A.D.I. steps to reach convergence on the parameter λ^{-1} in the case when $\mathrm{Ra} = 10^5$ and $h = 1/16$.

Suppose that for a particular value of the Rayleigh number the problem has been solved numerically on a grid of mesh size h. To find the solution on a grid of mesh size $\frac{1}{2}h$ we use the best available information to begin the new calculation, i.e., we use as our initial approximation values interpolated from those obtained on the coarser grid. Cubic interpolation is used for values of ψ and linear interpolation for values of T.

The average value of the Nusselt number is calculated using the trapezoidal rule, where we use the following approximation to the normal derivative of T on the hot wall:

$$\frac{\partial T}{\partial n}(0, z) = \frac{\{-3T(0, z) + 4T(h, z) - T(2h, z)\}}{2h}.$$

Table II contains the average Nusselt number on the hot wall and the maximum and minimum local Nusselt numbers on the hot wall, and their location. Table III contains the number D.A.D.I. steps and the run time, in seconds, required to reach the convergence criterion. The results were obtained on the Oxford University *ICL* 2980 computer. Contours for the temperature and stream function are shown in Figs. 2 to 9 for different values of the Rayleigh number.

TABLE II

Heat Transfer Results

Ra	Mesh	Average Nusselt Number	Maximum Nusselt Number		Minimum Nusselt Number	
		Nu	Nu_{max}	@ $z =$	Nu_{min}	@ $z =$
	17×17	1.120	1.515	0.86	0.697	0.00
10^3	33×33	1.118	1.508	0.91	0.693	0.00
	65×65	1.118	1.507	0.91	0.692	0.00
	17×17	2.357	3.838	0.81	0.615	0.00
10^4	33×33	2.270	3.628	0.84	0.592	0.00
	65×65	2.250	3.554	0.86	0.587	0.00
	17×17	5.146	8.423	0.88	0.854	0.00
10^5	33×33	4.758	8.508	0.91	0.755	0.00
	65×65	4.573	7.972	0.92	0.735	0.00
10^6	33×33	10.062	19.085	0.91	0.926	0.03
	65×65	9.272	19.590	0.95	0.999	0.00

TABLE III

Computational Details

Ra	Mesh	Number of D.A.D.I. Steps	Time
	17×17	24	4.9
10^3	33×33	19	14.9
	65×65	9	30.3
	17×17	36	6.7
10^4	33×33	36	26.9
	65×65	21	66.0
	17×17	111	21.1
10^5	33×33	92	68.9
	65×65	49	147.5
10^6	33×33	362	268.5
	65×65	335	1012.0

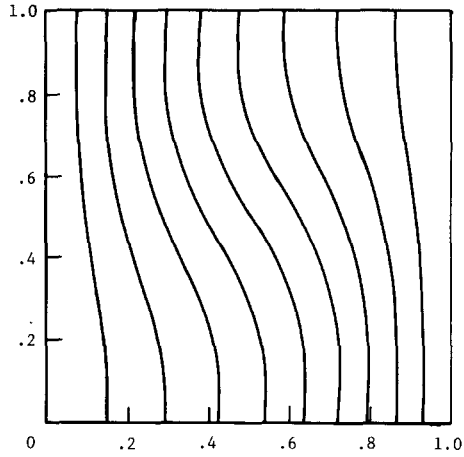

FIG. 2. Temperature contours for $Ra = 10^3$. Contour levels are 0.1 (0.1) 0.9.

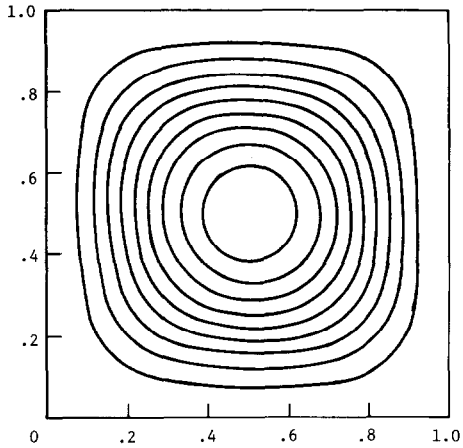

FIG. 3. Stream function contours for $Ra = 10^3$. Contour levels are -0.12 (-0.12) -1.08.

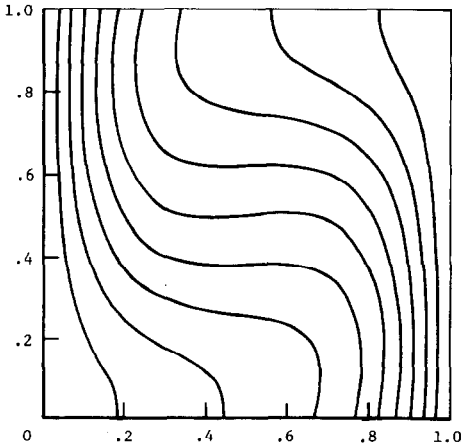

FIG. 4. Temperature contours for $Ra = 10^4$. Contour levels are 0.1 (0.1) 0.9.

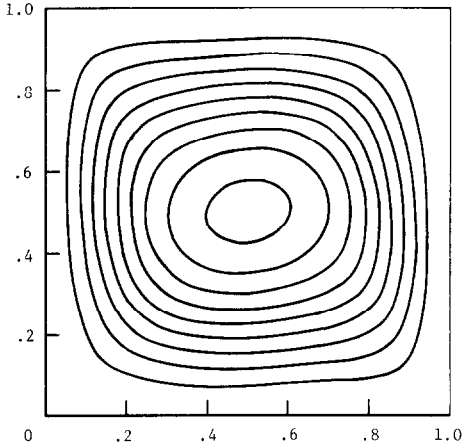

FIG. 5. Stream function contours for $Ra = 10^4$. Contour levels are -0.552 (-0.552) -4.968.

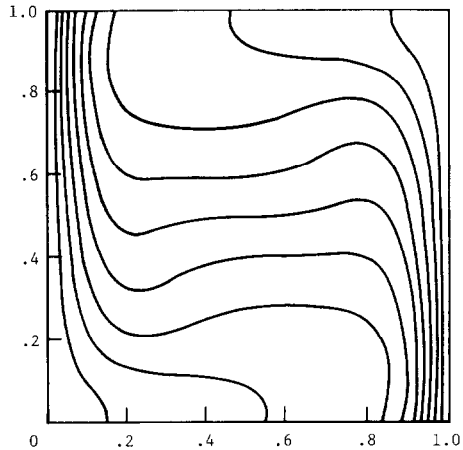

FIG. 6. Temperature contours for $Ra = 10^5$. Contour levels are 0.1 (0.1) 0.9.

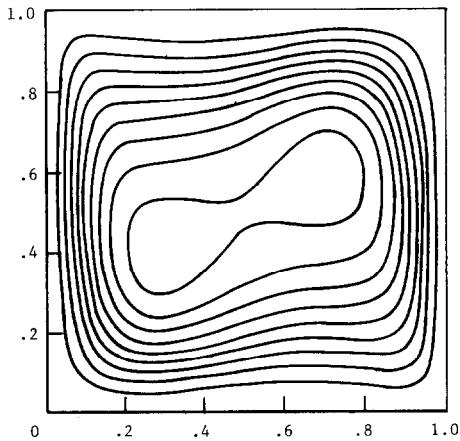

FIG. 7. Stream function contours for $Ra = 10^5$. Contour levels are -1.06 (-1.06) -9.54.

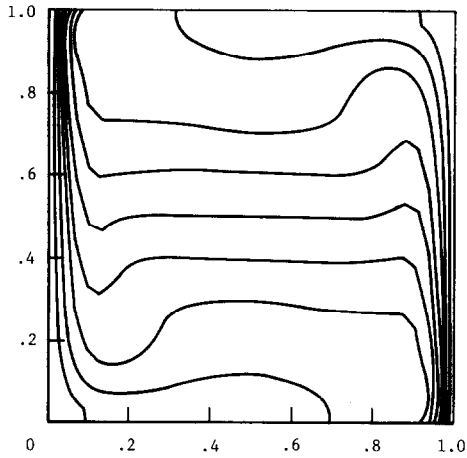

FIG. 8. Temperature contours for Ra = 10^6. Contour levels are 0.1 (0.1) 0.9.

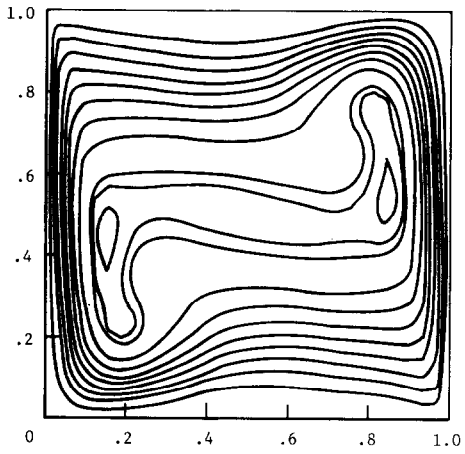

FIG. 9. Stream function contours for Ra = 10^6. Contour levels are -2.1 (-2.1) -18.9, -19.3, -19.8.

In Table IV we give the details of the experiments performed with Richardson extrapolation. The experiments were carried out for two values of the Rayleigh number, 10^3 and 10^5, on a 17×17 mesh. The results show that although some improvement in the method is made when the parameter α takes the value 0.9 the amount is not significant.

Experiments were also performed with different initial conditions to test the robustness of the method. The algorithm was run with various initial conditions including ones which were oscillatory and ones which were randomly generated with no deterioration in the performance of the method.

The step size Δt constantly changes during the calculations, its value rarely being the same for consecutive D.A.D.I. steps.

TABLE IV

Variation of Number of D.A.D.I. Steps with α and Ra

α	$Ra = 10^3$	$Ra = 10^5$
1.0	24	111
0.9	22	103
0.7	23	109
0.5	25	117

The results we have obtained mainly show a good agreement and the convergence is approximately quadratic. Also it is clear that some form of non-uniform grid is needed to resolve the boundary layers accurately when Ra is large. In the next section we show that this technique has the effect of improving the rate D.A.D.I. convergence.

7. Non-Uniform Grids

For large values of the Rayleigh number the flows develop strong boundary layers. This effect can be seen in Fig. 9, for example. When $Ra = 10^6$ we have had to use an extremely fine mesh, 65×65, in order to resolve these boundary layers. This is rather wasteful since the grid points are also densely distributed away from these layers where they are not needed. Here we apply the technique of Kalnáy de Rivas [8] to resolve the boundary layers using a non-uniform grid.

Basically, the idea is to make a change of independent variable so that the domain is mapped into a new co-ordinate system where the variations of the solution are not so rapid. The grid intervals are varied by defining stretched co-ordinates ζ and η such that $x = x(\zeta)$ and $z = z(\eta)$, where the grid intervals $\Delta\zeta$ and $\Delta\eta$ are constant and x and z are the old physical co-ordinates. The mapping is chosen so that the solution, when regarded as a function of the new variables, has no boundary layers.

Kalnáy de Rivas [8] and Jones and Thompson [7] show how to express derivatives in terms of the stretched co-ordinates. For example, we can express the first derivative in terms of ζ in the following manner

$$\frac{\partial v}{\partial x} = \frac{\partial v}{\partial \zeta} \cdot \frac{d\zeta}{dx}. \tag{23}$$

Equation (23) can be discretized using central differences to give the following approximation

$$\frac{\partial v}{\partial x} \simeq \frac{v_{i+1,j} - v_{i-1,j}}{2\Delta\zeta} \left.\frac{d\zeta}{dx}\right|_{x_i}, \tag{24}$$

where $v_{i,j}$ is the value of v at the grid point (x_i, z_j) with $x_i = x(i\Delta\zeta)$ and $z_j = z(j\Delta\eta)$.

The transformation can be differentiated using central differences to obtain the following approximation to the first derivative:

$$\frac{\partial v}{\partial x} \simeq \frac{(v_{i+1,j} - v_{i-1,j})}{2\Delta\zeta} \cdot \frac{2\Delta\zeta}{(x_{i+1} - x_{i-1})} = \frac{(v_{i+1,j} - v_{i-1,j})}{(x_{i+1} - x_{i-1})}. \tag{25}$$

Finite difference approximations for higher order derivatives are obtained in a similar way.

Let $x(\zeta)$ and $z(\eta)$ be two grid stretching functions with constant grid intervals $\Delta\zeta$ and $\Delta\eta$, respectively. The region Ω is covered with a variable grid defined by the above mappings. We define $T_{i,j}$ and $\psi_{i,j}$ to be the values of $T(x, z)$ and $\psi(x, z)$ respectively at the grid point (x_i, z_j). The finite difference equations are constructed using approximations like Eq. (25) for the derivatives. The system of finite difference equations are solved using the D.A.D.I. method described earlier.

The problem is solved on the following non-uniform grids:

(a)
$$x(\zeta) = \sin^2(\tfrac{1}{2}\pi\zeta),$$
$$z(\eta) = \sin^2(\tfrac{1}{2}\pi\eta). \tag{26}$$

(b)
$$x(\zeta) = 6\zeta^5 - 15\zeta^4 + 10\zeta^3,$$
$$z(\eta) = 6\eta^5 - 15\eta^4 + 10\eta^3. \tag{27}$$

These grid stretching functions give a smaller spacing of the grid points near the boundary.

The problem was solved for Rayleigh numbers of 10^5 and 10^6 on the non-uniform grids defined by Eqs. (26) and (27) with $\Delta\zeta = \Delta\eta = 0.04$. In Table V we compare the average value of the Nusselt number along the hot wall obtained on these non-uniform grids, a uniform 26×26 mesh and a uniform 65×65 mesh. In Tables VI and VII we compare the number of D.A.D.I. steps and run time, respectively, to reach the convergence criterion, which is the same as that used for the results in Table III.

In Table V we see that we have obtained a good estimate of the Nusselt number

TABLE V

Average Value of the Nusselt Number

		Stretched Mesh		
Ra	Uniform Mesh 26×26	(a) 26×26	(b) 26×26	Uniform Mesh 65×65
10^5	4.889	4.596	4.595	4.573
10^6	10.163	9.123	9.066	9.272

TABLE VI

Number of D.A.D.I. Steps

Ra	Uniform Mesh 26×26	Stretched Mesh (a) 26×26	Stretched Mesh (b) 26×26	Uniform Mesh 65×65
10^5	151	85	84	80
10^6	676	334	369	426

by using a stretched grid even though we have only a 26×26 mesh. For small values of the Rayleigh number the use of a stretched grid has little effect. It is only when the Rayleigh number becomes large that we obtain an improvement by using non-uniform grids. The use of non-uniform grids to resolve the boundary layers has had the effect of improving the rate of D.A.D.I. convergence. Approximately twice as many steps of D.A.D.I. were required for convergence of the method using the uniform 26×26 mesh than for stretched 26×26 meshes.

The use of non-uniform grids has allowed us to resolve the boundary layers using comparatively few mesh points. Reasonable accuracy has also been obtained on the stretched grids compared with an extremely fine mesh.

The iterative solution of finite difference equations constructed on a non-uniform grid usually presents great difficulties. This is due to the problem of finding suitable parameters for the acceleration of convergence of any selected iterative method. Hence, an advantage of the D.A.D.I. method over standard iterative methods for solving problems of this type is that we do not require an a priori choice of parameters to accelerate convergence.

TABLE VII

Computational Time

Ra	Uniform Mesh 26×26	2400 Stretched Mesh (a) 26×26	2400 Stretched Mesh (b) 26×26	Uniform Mesh 65×65
10^5	68	85	84	238
10^6	299	332	364	1280

8. SUMMARY

In this paper we have shown how the D.A.D.I. method can be implemented to solve the natural convection problem. After eliminating the vorticity, which avoids the need for a vorticity boundary condition, we converted the equations to parabolic form enabling us to march in time to the steady state solution. The rate of convergence to steady state has been enhanced by using different time steps for the two equations.

The D.A.D.I. method which uses an automatic step size changer has eliminated the usual problem associated with nonlinear equations and non-uniform grids of finding a priori parameters to accelerate convergence. The strategy also recognizes instabilities as they begin to occur and bypasses them by decreasing Δt. Boundary layers have been resolved efficiently using non-uniform grids with good results.

ACKNOWLEDGMENT

I would like to thank Ian Jones for introducing me to this problem.

REFERENCES

1. S. CONTE AND R. J. DAMES, *Math. Tables Aids Comput.* **12** (1958), 198–205.
2. S. DOSS AND K. MILLER, *SIAM J. Numer. Anal.* **16** (1979), 837–856.
3. J. DOUGLAS AND H. H RACHFORD, *Trans. Amer. Math. Soc.* **82** (1956), 421–439.
4. I. P. JONES, *J. Fluid Mech.* **95** (1979), 4, inside back cover.
5. I. P. JONES, *Num. Heat Transf.* **2** (1979), 193–213.
6. I. P. JONES, A comparison problem for numerical methods in fluid dynamics: the "double glazing" problem, *in* "Numerical Methods in Thermal Problems" (R. W. Lewis and K. Morgan, Eds.), Pineridge Press, Swansea, U.K., 1979.
7. I. P. JONES AND C. P. THOMPSON, "On the Use of Non-uniform Grids in Finite Difference Calculations," A.E.R.E. Harwell Report R.9765, H.M.S.O., London, 1980.
8. E. KALNAY DE RIVAS, *J. Comput. Phys.* **10** (1972), 202–210.
9. G. D. MALLINSON AND G. DE VAHL DAVIS, *J. Comput. Phys.* **12** (1973), 435–461.
10. G. D. MALLINSON AND G. DE VAHL DAVIS, *J. Fluid Mech.* **83** (1977), 1, 1–31.
11. D. W. PEACEMAN AND H. H. RACHFORD, *J. Soc. Indust. Appl. Math.* **3** (1955), 28–41.